8-1-2015

Pharmacodynamics of folic acid receptor targeted antiretroviral nanotherapy in HIV-1-infected humanized mice.

Pavan Puligujja
University of Nebraska Medical Center

Mariluz Araínga
University of Nebraska Medical Center, m.araingaramirez@unmc.edu

Prasanta Dash
University of Nebraska Medical Center, pdash@unmc.edu

Diana L. Palandri
University of Nebraska Medical Center, diana.palandri@unmc.edu

R. Lee Mosley
University of Nebraska Medical Center, Omaha, NE, rlmosley@unmc.edu

Antiviral Research 120 (2015) 85–88

Contents lists available at ScienceDirect

Antiviral Research

journal homepage: www.elsevier.com/locate/antiviral

Short Communication

Pharmacodynamics of folic acid receptor targeted antiretroviral nanotherapy in HIV-1-infected humanized mice

Pavan Puligujja, Mariluz Araínga, Prasanta Dash, Diana Palandri, R. Lee Mosley, Santhi Gorantla, Larisa Poluektova, JoEllyn McMillan, Howard E. Gendelman *

Department of Pharmacology and Experimental Neuroscience, University of Nebraska Medical Center, Omaha, NE 68198-5880, USA

ARTICLE INFO

Article history:
Received 19 April 2015
Revised 22 May 2015
Accepted 24 May 2015
Available online 27 May 2015

Keywords:
Folic acid receptor
Long-acting nanoformulated antiretroviral therapy
Human immunodeficiency virus type one
Pharmacokinetics
Pharmacodynamics
Non-obese diabetic severe combined immunodeficient mice

ABSTRACT

Long-acting nanoformulated antiretroviral therapy (nanoART) can sustain plasma drug levels and improve its biodistribution. Cell targeted-nanoART can achieve this and bring drug efficiently to viral reservoirs. However, whether such improvements affect antiretroviral responses remains unknown. To these ends, we tested folic acid (FA)-linked poloxamer407-coated ritonavir-boosted atazanavir (FA-nanoATV/r) nanoparticles for their ability to affect chronic HIV-1 infection in humanized mice. Following three, 100 mg/kg FA-nanoATV/r intramuscular injections administered every other week to infected animals, viral RNA was at or below the detection limit, cell-associated HIV-1p24 reduced and CD4+ T cell counts protected. The dosing regimen improved treatment outcomes more than two fold from untargeted nanoATV/r. We posit that these nanoformulations have potential for translation to human use.

Combination antiretroviral therapy can reduce, but not eliminate, human immunodeficiency virus (HIV) replication. Therapeutic limitations, including adherence to therapeutic regimens and inadequate drug penetration to viral reservoirs can lead to treatment failures. To this end, our laboratories developed long-acting antiretroviral nanoformulations (nanoART). These were demonstrated to improve antiviral activities (Balkundi et al., 2011). Weekly parenteral administration of poloxamer188 formulated ritonavir-boosted atazanavir (P188-ATV/r) for 6 weeks provided up to a 3-log viral load reduction in humanized HIV-1 infected NOD/scid-IL-2Rγc^{null} (NSG) mice (Dash et al., 2012). Despite these pharmacodynamics (PD) advantages, high dose, volume of injection and dosing frequency precluded nanoART translation to human use (Gautam et al., 2013; Nowacek et al., 2010; Roy et al., 2012). Such limitations were compounded by injection site irritations and high dose volume required to achieve plasma ATV/r levels sufficient for viral inhibition (Gautam et al., 2013). In order to reduce dose and injection volume, we developed a folic acid (FA) modification approach to target the folate receptor on macrophages (Puligujja et al., 2013). The advantage in antiviral activity of FA-nanoATV/r was demonstrated in NSG mice following pre-exposure prophylaxis (PrEP) regimens. The present study on FA-nanoATV/r treated NSG mice builds on prior pharmacokinetic (PK) and PD studies. The promising results lay a foundation to further develop nanoformulations for clinical use (Puligujja et al., 2015).

1. Physicochemical characterization

FA-nanoATV/r nanoformulations (FA-P407-ATV/r) were prepared by high-pressure homogenization (Puligujja et al., 2013). Physicochemical characteristics including particle size, charge, polydispersity (PDI) and shape were determined. Particle size, polydispersity and zeta potential ranged from 257 to 433 nm, 0.17 to 0.33 and −8.9 to −12.1 mV, respectively for FA-nanoATV and FA-nanoRTV.

2. Infection and nanoART treatments

The University of Nebraska Medical Center Institutional Review Board approved human fetal tissue usage. CD34+ hematopoietic stem cells (HSC) were isolated from human fetal liver by immune selection (Miltenyl Biotec Inc., Auburn, CA) then transplanted into NSG mice at birth (Gorantla et al., 2007). At 22 weeks of age mice were infected with a 10^4 tissue culture infective dose 50

* Corresponding author at: Department of Pharmacology and Experimental Neuroscience, 985880 Nebraska Medical Center, Omaha, NE 68198-5880, USA.
E-mail address: hegendel@unmc.edu (H.E. Gendelman).

http://dx.doi.org/10.1016/j.antiviral.2015.05.009
0166-3542/

($TCID_{50}$)/mouse of HIV-1_{ADA} by intraperitoneal injection. Ten weeks later mice were administered 100 mg/kg FA-nanoATV/r intramuscularly with booster doses at 2 and 4 weeks. Replicate animals were untreated. All mice were sacrificed at week 6. Mice were maintained on a folate deficient diet from 2 weeks before and throughout the study. This enabled serum folate levels of <25 nM that are comparable to humans (Fig. 1A).

3. Plasma and tissue drug distribution

Plasma samples were collected at weeks 2, 4 and 6 after drug administration. Mouse tissues were collected after sacrifice. Drug concentrations were determined by ultra-performance liquid chromatography–tandem mass spectrometry (UPLC–MS/MS) (Huang et al., 2011). Following treatment with FA-nanoATV/r, plasma ATV concentrations were maintained above the human minimum effective concentration (MEC) of 150 ng/ml (la Porte et al., 2006) throughout the study. At 2, 4 and 6 weeks ATV levels were 285 ± 84, 701 ± 128 and 404 ± 101 ng/ml respectively. Corresponding plasma RTV concentrations were 126 ± 65, 139 ± 27 and 46 ± 13 ng/ml respectively (Fig. 1B). Tissue drug levels in liver, lung, spleen and kidney were 3835 ± 792, 250 ± 95, 69 ± 14 and 374 ± 72 ng/g for ATV and 2407 ± 554, 171 ± 90, 289 ± 93 and 452 ± 136 ng/g for RTV respectively (Fig. 1C).

A

Group name	Infection time	Dose	Number of doses	Treatment schedule	Sacrifice	Total amount of drug administered
FA-P407-ATV/r	10 weeks	100 mg/kg	3	Weeks 0, 2 and 4 after infection (3 doses)	Week 6 after infection	300 mg
P407-ATV/r	10 weeks	250 mg/kg	3	Weeks 0, 1 and 2 after infection	Week 4 after infection	750 mg
[a]P188-ATV/r	8 weeks	250 mg/kg	6	Weeks 0, 1, 2, 3, 4, 5 after infection	Week 6 after infection	1500 mg

[a]Previously reported data

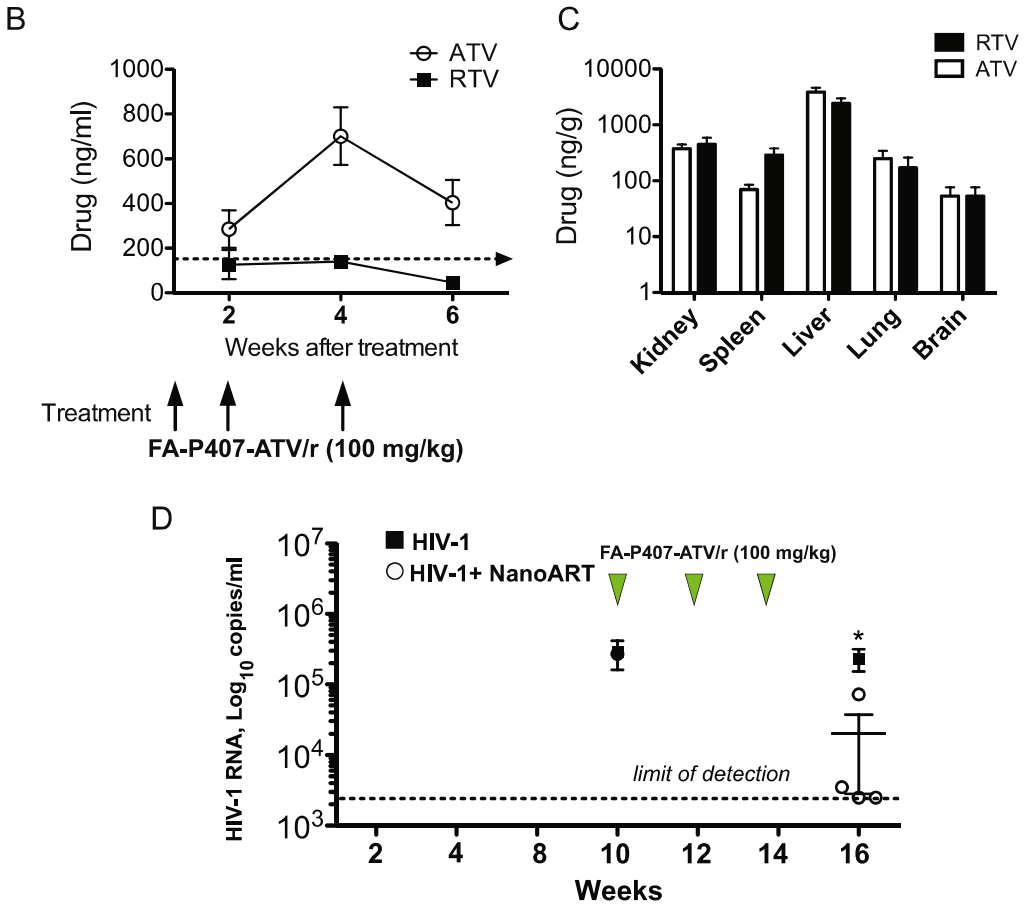

Fig. 1. Comparison of pharmacokinetics and viral loads between targeted and untargeted nanoformulations in CD34+ hematopoietic stem cell-transplanted humanized NOD/scid-IL-2Rγc^{null} mice. (A) Table describing the infection and treatment scheme in FA-P407-ATV/r and untargeted groups. FA-P407-ATV/r (100 mg/kg) was administered after the mice were infected for 10 weeks. A boosting dose of 100 mg/kg was again administered 2 and 4 weeks following the initial dose. Plasma was collected at indicated time points. (B) ATV (open circles) and RTV (closed boxes) concentrations in plasma were determined by UPLC–MS/MS. Tissues were collected 6 weeks following the initial dose. Data are expressed as mean ± SEM ($n = 5$). (C) Tissue ATV and RTV concentrations were determined by UPLC–MS/MS. All data are expressed as mean ± SEM ($n \geqslant 3$). (D) Plasma viral load in CD34+ HSC-NSG mice during and following FA-P407-ATV/r treatment. Humanized NSG mice were either treated with 3 doses of 100 mg/kg FA-P407-ATV/r at 10, 12 and 14 weeks or were untreated following HIV-1 infection. Plasma viral loads from FA-P407-ATV/r (open circles) and untreated (closed boxes) groups were determined before and after treatment as illustrated. Data are expressed, as mean ± SEM. Data are statistically significant at $P < 0.05$ with Mann–Whitney test ($n \geqslant 4$).

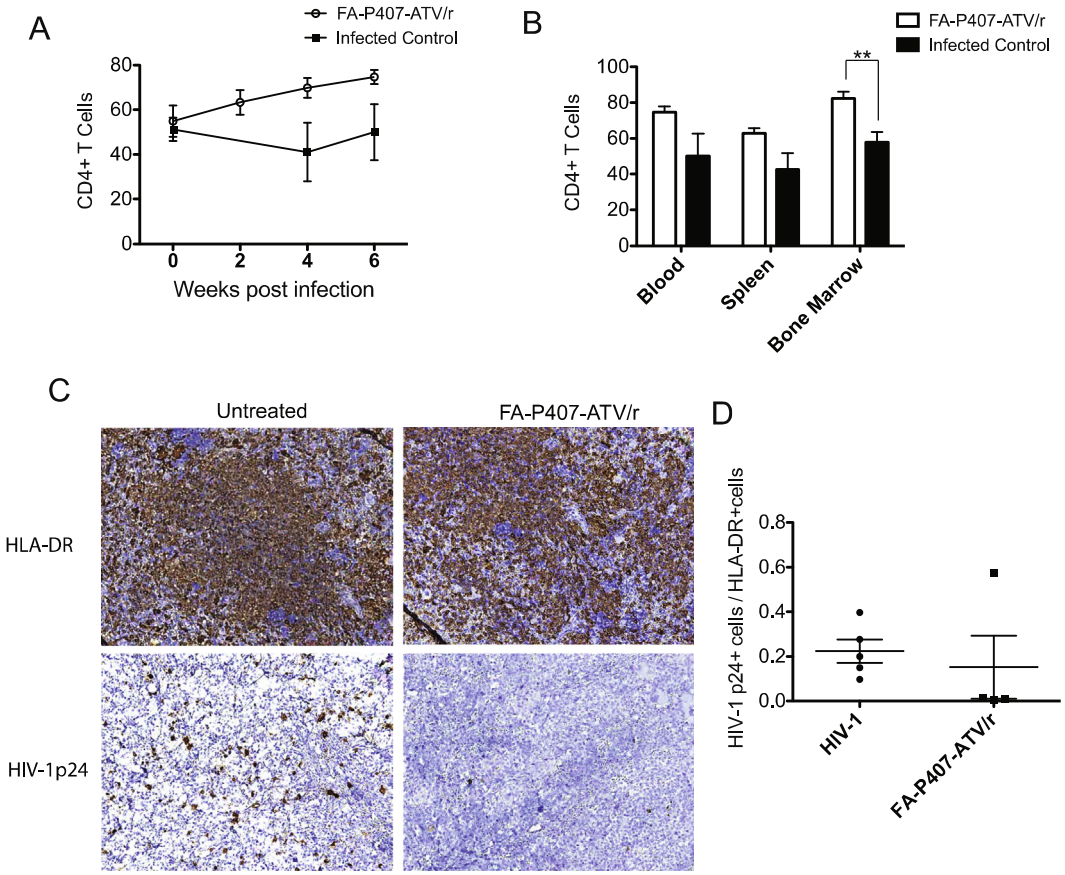

Fig. 2. Pharmacodynamics of FA-P407-ATV/r treatment in CD34+ hematopoietic stem cell-transplanted NSG mice. The percent of CD4+ T cells among CD3+ T cells were determined using fluorescence-activated cell sorting between treated (open box) and untreated infected control (closed box) groups. (A) CD4+ T cells in blood during the study and (B) CD4+ T cells in blood, spleen and bone marrow at the end of the study. Data are expressed as mean ± SEM. **Statistically different at $P < 0.01$ using unpaired Student's *t*-test ($n = 5$). Spleen immunohistochemistry was performed for HIV-1p24 antigens following FA-P407-ATV/r treatment. Humanized NSG mice were infected with HIV-1_{ADA} for 10 weeks and then treated with 100 mg/kg FA-P407-ATV/r at 0, 2 and 4 weeks. (C) Spleens were collected from treated and untreated groups and immunostained with antibodies for either HLA-DR or HIV-1p24, then visualized with DAB staining. (D) Antiretroviral efficacy was determined by counting the number of HIV-1p24+ cells and HLA-DR+ cells from five random microscopic fields per mouse and then calculating the HIV-1p24+ to HLA-DR+ cell ratios. Data are expressed, as mean ± SEM ($n \geqslant 4$).

4. Viral load determinations

To determine antiviral efficacy of FA-nanoATV/r, pre- and post-treatment viral loads were determined in blood from HIV-1 infected-CD34+ HSC-NSG mice. Viral load (RNA copies/ml) was determined in plasma using COBAS Amplicor System v1.5 kit (Roche Molecular Diagnostics, Switzerland) (Dash et al., 2012). Individual mouse viral loads before treatment with FA-nanoATV/r were 0.7×10^5, 5.0×10^5, 2.0×10^5, 3.2×10^5, and 0.7×10^5 viral RNA copies/ml. Treatment with FA-P407-ATV/r produced up to 3 log decrease in the viral load and was statistically significant at $P < 0.05$ with Mann–Whitney test (Fig. 1D); with 2 mice showing undetectable viral RNA, one with a 2-log decrease (3×10^3 viral RNA copies/ml) and the fourth exhibiting a log decrease (7×10^4 viral RNA copies/ml). The variance in viral levels is likely attributable to humanization, mouse–human cell biology and drug biodistribution differences and irradiation-associated toxicities. The average post-infection and post-treatment viral loads for the untreated group were 2.9×10^5 and 2.2×10^5 viral RNA copies/ml.

5. Flow cytometric analyses

To assess whether FA-nanoATV/r treatment provided immune protection, we determined the percent of human CD45, CD3, CD4 and CD8 positive cells in blood, spleen and bone marrow. The number of human CD45+, CD3+, CD4+ and CD8+ cells (BD Pharmingen, San Diego, CA) were determined by fluorescence-activated cell sorting (FACS) using a BD FACSDiva® (BD Immunocytometry Systems, Mountain View, CA) system. CD4+ lymphocyte percentages were determined from the CD3+ gated cells. After sacrifice, CD4+ and CD8+ T cell percentages were calculated from CD45+ cells; total CD3+ cell number was considered to be the sum of CD4+ and CD8+ cell numbers.

The average pre-infection CD4+ T cell percentages among the untreated and FA-nanoATV/r treated groups in blood were 54.8 ± 7.1% and 51.2 ± 5.2% of the CD3+ T cell population, respectively. After the initial 100 mg/kg dose the average CD4+ T cell percentage in blood was 63.0 ± 5.5% at 2 weeks post treatment. A second dose was administered at week 2 and CD4+ T cell percentages in blood increased to 69.8 ± 4.4% at week 4. After the third dose CD4+ T cell percentages increased further to 74.7 ± 3.1% at week 6. In contrast, the CD4+ T cell percentages in infected and untreated mice dropped to 50.0 ± 12.5% at week 6 (Fig. 2A). The uninfected and untreated mice had CD4+ T cell percentages of 73.5 ± 3.9%. The CD4+ T cell percentages in spleen and bone marrow were 62.7 ± 2.9% and 82.3 ± 3.8% for the FA-nanoATV/r group and 42.5 ± 9.1% and 57.8 ± 5.7% for the infected and untreated mice (Fig. 2B). Moreover, the CD4+ T cell percentages in uninfected and untreated mice in spleen and bone marrow were 62.4 ± 2.9% and 90.2 ± 1.7%. The corresponding CD4:CD8 T cell ratios in blood, spleen and bone marrow are shown in Supplementary Fig. 1A and B.

6. Immunohistochemistry

Spleens collected at sacrifice were fixed with 10% neutral buffered formalin (Fisher Scientific, Kalamazoo, MI) and paraffin embedded. Five μm thick serial sections were collected and immunostained (Fig. 2C) with human leukocyte antigen; HLA-DR (clone CR3/43; 1:100) and mouse monoclonal antibody against HIV-1p24 (clone Kal-1; 1:10) (Puligujja et al., 2015). Antiretroviral activity was determined by dividing the total HIV-1p24+ cells by total HLA-DR+ cells in five random microscopic fields/mouse. The ratio of HIV-1p24+ cells among HLA-DR+ cells in spleen was 0.15 ± 0.14 for the FA-nanoATV/r group compared to 0.22 ± 0.05 in the untreated mice (Fig. 2D).

There is a significant interest for the development of long-acting ART nanoformulations (Dolgin, 2014). Although these show improved drug PK and tissue distribution, the relatively high dose and volume of injection remain a limitation. FA-nanoATV/r was improved over non-targeted formulations in both these parameters (Puligujja et al., 2013). For the latter, the PD efficacy of FA-nanoATV/r in a PrEP regimen protected humanized mice against acute HIV infection (Puligujja et al., 2015). However the efficacy of FA-nanoATV/r in treating chronic HIV-1 infection was not investigated. Thus, we evaluated PD outcomes of FA-nanoATV/r in chronically HIV-1 infected CD34+ HSC-NSG mice.

Targeted FA-P407-ATV/r improved the drug-dosing regimens (Dash et al., 2012). FA-P407-ATV/r provided a significant decrease in viral loads compared to untreated infected mice ($P < 0.05$, Mann–Whitney test). It is known that higher plasma drug concentrations are needed for efficient antiviral responses (Winston et al., 2005). The plasma ATV levels following FA-P407-ATV/r were above the MEC. Additionally, in comparison with untargeted P407-ATV/r (Supplementary Fig. 2), FA-P407-ATV/r treatments showed enhanced viral load suppression. This can be attributed again to the enhanced plasma drug concentrations with FA targeting. Although the dosing regimen was not identical between the studies, the suppression in viral load supports the potential of FA-P407-ATV/r to reduce dosing frequencies.

We reported previously on the antiviral activity of nanoART in CD34+ NSG mice (Dash et al., 2012). In that study CD34+ HSC-NSG were infected for 8 weeks and treated weekly for 6 weeks with 250 mg/kg P188-ATV/r. The mice were sacrificed 7 weeks after the first dose. We compared the viral loads from this previously published study with the viral loads after FA-nanoATV/r treatment (Fig. 1D). In comparison to the P188-ATV/r study, the dose of 100 mg/kg FA-nanoATV/r was 2.5 times less than what was administered with P188-ATV/r. Also, the frequency of FA-nanoATV/r treatment was half the frequency of the P188-ATV/r treatment. Taken together, FA-nanoATV/r treatment with 5 times less total drug than P188-ATV/r was sufficient to reduce the viral load to undetectable levels. The effectiveness of FA targeting enables FA-nanoATV/r to be administered once every 2 weeks.

Flow cytometry analysis in blood, spleen and bone marrow demonstrated CD4+ T cell count drops after 10 weeks of HIV-1 infection. These then returned gradually to uninfected levels after treatment. Although not statistically significant, immunohistochemical staining for HIV-1p24 antigen in spleen after FA-nanoATV/r treatment decreased over time. These results demonstrate the potential of FA-nanoATV/r to treat a chronic viral infection. Recent phase II studies underway for monthly or every other month antiretroviral drug injections will permit future development of folic acid targeting of longer acting antiretrovirals.

Acknowledgments

This work was supported by the University of Nebraska Foundation which includes individual donations from Carol Swarts and Frances and Louie Blumkin, the Vice Chancellor's office of the University of Nebraska Medical Center, ViiV Healthcare and National Institutes of Health grants P01 DA028555, R01 NS36126, P01 NS31492, 2R01 NS034239, P01 MH64570, P01 NS43985, P30 MH062261 and R01 AG043540. The authors thank Jaclyn Knibbe, Selena Dickinson and Edward Makarov for expert technical assistance.

Appendix A. Supplementary data

Supplementary data associated with this article can be found, in the online version, at http://dx.doi.org/10.1016/j.antiviral.2015.05.009.

References

Balkundi, S., Nowacek, A.S., Veerubhotla, R.S., Chen, H., Martinez-Skinner, A., Roy, U., Mosley, R.L., Kanmogne, G., Liu, X., Kabanov, A.V., Bronich, T., McMillan, J., Gendelman, H.E., 2011. Comparative manufacture and cell-based delivery of antiretroviral nanoformulations. Int. J. Nanomed. 6, 3393–3404.

Dash, P.K., Gendelman, H.E., Roy, U., Balkundi, S., Alnouti, Y., Mosley, R.L., Gelbard, H.A., McMillan, J., Gorantla, S., Poluektova, L.Y., 2012. Long-acting nanoformulated antiretroviral therapy elicits potent antiretroviral and neuroprotective responses in HIV-1-infected humanized mice. Aids 26, 2135–2144.

Dolgin, E., 2014. Long-acting HIV drugs advanced to overcome adherence challenge. Nat. Med. 20, 323–324.

Gautam, N., Roy, U., Balkundi, S., Puligujja, P., Guo, D., Smith, N., Liu, X.M., Lamberty, B., Morsey, B., Fox, H.S., McMillan, J., Gendelman, H.E., Alnouti, Y., 2013. Preclinical pharmacokinetics and tissue distribution of long-acting nanoformulated antiretroviral therapy. Antimicrob. Agents Chemother. 57, 3110–3120.

Gorantla, S., Sneller, H., Walters, L., Sharp, J.G., Pirruccello, S.J., West, J.T., Wood, C., Dewhurst, S., Gendelman, H.E., Poluektova, L., 2007. Human immunodeficiency virus type 1 pathobiology studied in humanized BALB/c-Rag2−/−gammac−/− mice. J. Virol. 81, 2700–2712.

Huang, J., Gautam, N., Bathena, S.P., Roy, U., McMillan, J., Gendelman, H.E., Alnouti, Y., 2011. UPLC–MS/MS quantification of nanoformulated ritonavir, indinavir, atazanavir, and efavirenz in mouse serum and tissues. J. Chromatogr. B, Anal. Technol. Biomed. Life Sci. 879, 2332–2338.

Nowacek, A.S., McMillan, J., Miller, R., Anderson, A., Rabinow, B., Gendelman, H.E., 2010. Nanoformulated antiretroviral drug combinations extend drug release and antiretroviral responses in HIV-1-infected macrophages: implications for neuroAIDS therapeutics. J. Neuroimmune Pharmacol. 5, 592–601.

la Porte, C.J.L., Black, D.J., Blaschke, T., Boucher, C.A.B., Fletcher, C.V., Flexner, C., Gerber, J., Kashuba, A.D.M., Schapiro, J.M., Burger, D.M., 2006. Updated guideline to perform therapeutic drug monitoring for antiretroviral agents. Rev. Antivir. Ther. 2006, 4–14.

Puligujja, P., McMillan, J., Kendrick, L., Li, T., Balkundi, S., Smith, N., Veerubhotla, R.S., Edagwa, B.J., Kabanov, A.V., Bronich, T., Gendelman, H.E., Liu, X.M., 2013. Macrophage folate receptor-targeted antiretroviral therapy facilitates drug entry, retention, antiretroviral activities and biodistribution for reduction of human immunodeficiency virus infections. Nanomed. Nanotechnol. Biol. Med. 9, 1263–1273.

Puligujja, P., Balkundi, S.S., Kendrick, L.M., Baldridge, H.M., Hilaire, J.R., Bade, A.N., Dash, P.K., Zhang, G., Poluektova, L.Y., Gorantla, S., Liu, X.M., Ying, T., Feng, Y., Wang, Y., Dimitrov, D.S., McMillan, J.M., Gendelman, H.E., 2015. Pharmacodynamics of long-acting folic acid-receptor targeted ritonavir-boosted atazanavir nanoformulations. Biomaterials 41, 141–150.

Roy, U., McMillan, J., Alnouti, Y., Gautum, N., Smith, N., Balkundi, S., Dash, P., Gorantla, S., Martinez-Skinner, A., Meza, J., Kanmogne, G., Swindells, S., Cohen, S.M., Mosley, R.L., Poluektova, L., Gendelman, H.E., 2012. Pharmacodynamic and antiretroviral activities of combination nanoformulated antiretrovirals in HIV-1-infected human peripheral blood lymphocyte-reconstituted mice. J. Infect. Dis. 206, 1577–1588.

Winston, A., Bloch, M., Carr, A., Amin, J., Mallon, P.W., Ray, J., Marriott, D., Cooper, D.A., Emery, S., 2005. Atazanavir trough plasma concentration monitoring in a cohort of HIV-1-positive individuals receiving highly active antiretroviral therapy. J. Antimicrob. Chemother. 56, 380–387.